Development of Highly Sensitive Optical Nanoantenna for Bacterial Detection

Journal:	*Analyst*
Manuscript ID	AN-ART-03-2022-000475.R1
Article Type:	Paper
Date Submitted by the Author:	08-Apr-2022
Complete List of Authors:	Itagaki, Satohiro; Osaka Prefecture University, Department of Applied Chemistry Tanabe, So; Osaka Prefecture University, Department of Applied Chemistry Ikeda, Hikaru; Osaka Prefecture University, Department of Applied Chemistry Shan, Xueling; Changzhou University Nishii, Shigeki; Osaka Prefecture University, Department of Applied Chemistry Yamamoto, Yojiro; Osaka Prefecture University, Department of Applied Chemistry Sadanaga, Yasuhiro; Osaka Prefecture University, Department of Applied Chemistry Chen, Zhidong; Changzhou University, Shiigi, Hiroshi; Osaka Prefecture University, Department of Applied Chemistry

SCHOLARONE™
Manuscripts

ARTICLE

Development of Highly Sensitive Optical Nanoantenna for Bacterial Detection

Satohiro Itagaki,[a] So Tanabe,[a] Hikaru Ikeda,[a] Xueling Shan,[b] Shigeki Nishii,[a] Yojiro Yamamoto,[a] Yasuhiro Sadanaga,[a] Zhidong Chen,[b] and Hiroshi Shiigi*[ac]

Gold nanoparticles (AuNPs) are chemically stable and serve as excellent labels because their characteristic red coloration based on the localized surface plasmon resonance (LSPR) does not fade. However, it is necessary to control the structure of AuNPs to use them as labels for various analyses, because their optical properties depend strongly on their size, shape, and state of aggregation. In this study, we developed gold nanostructures (AuNSs) by encapsulating many small AuNPs within a polymer for scattering light-based bacterial detection. The AuNSs consisting of many small nanoparticles provided stronger scattered light intensity than a single AuNP of the same particle size. We found that the aggregation of the AuNSs enhanced the scattering light intensity, depending strongly on their aggregation states, and did not affect the wavelength of the scattering light observed under a dark-field microscope. By specifically binding the antibody-introduced AuNSs to the antigen on the bacterial surface, it was possible to label the target bacteria and detect them based on their light scattering characteristics. In addition, to improve the accuracy of the selective identification of the cells of interest, labels based on scattered light should ideally have a fixed wavelength of scattered light with high intensity. From these perspectives, we developed a method of constructing an optical antenna on the surface of target bacterial cells using antibody-introduced NSs.

Introduction

Bacteria are important components of ecosystems and play an important role in our daily lives by supporting environmental purification, drug discovery, organic farming, and the production of functional foods.[1-3] However, some of these microbes, especially enterohemorrhagic *Escherichia coli*, can cause infections with serious adverse effects on the human body. These are extremely dangerous bacteria that can be fatal even at a level of ~100 cells in the human body and are the cause of most of the annual food poisoning cases worldwide.[4-8] Therefore, food factories that provide food to many consumers need to test their products for this pathogen before shipping. Currently, the identification and testing of these pathogens rely on colony counting methods in most sites.[9,10] However, bacterial testing, including culture, is time consuming (> 24 h). That is, the results are only available after the shipment has already been sent. Gram staining, a classic biological protocol for bacterial analyses using optical microscopy, is still in active use today.[11,12] However, gram staining protocols require long-term cell culture and cannot identify the bacterial species. Fluorescent labeling using a dye-conjugated antibody presents problems including short fluorescence signal lifetime.[13] Each bacterial testing method has its challenges. Therefore, new methods should be developed for rapid and easy bacterial evaluation and identification.

Gold nanoparticles (AuNPs), which have high electron density and high chemical stability, can be used in a variety of applications owing to their unique optical properties that depend on their size, shape, and aggregation.[14,15] The free electrons present on the AuNP surface produce localized surface plasmon resonance (LSPR) involving collective vibrations induced through interaction with visible light. Considering this, it should be possible to control the LSPR of a nanometer-scale antenna structure through the careful assembly of AuNPs.[16-19] The biomedical applications of AuNPs include the use of immunogold-labeled antibodies for cell detection through microscopy.[20] In this case, antibodies are generally introduced onto the AuNP surface via covalent bonds to establish a binding site. We previously described the development of a novel detection method that relies on the production of a highly sensitive optical antenna on the surface of a single bacterial cell using an immune antibody-enriched AuNP.[14,21] Under a dark-field microscope (DFM), AuNPs are observed as scattered light spots of different colors such as blue, white, or red. Therefore, it is necessary to develop

a. *Department of Applied Chemistry, Osaka Prefecture University, 1-1 Gakuen, Naka, Sakai, Osaka 599-8531, Japan.*
b. *Jiangsu Key Laboratory of Advanced Catalytic Materials and Technology, School of Petrochemical Engineering, Changzhou University, Changzhou 213164, China.*
c. *Osaka International Research Center for Infectious Diseases, 1-2 Gakuen, Naka, Sakai, Osaka 599-8570, Japan.*

nanostructures with stable optical properties that are unaffected by their aggregation state. In addition, for improving the accuracy of the selective identification of the cells of interest, labels based on scattered light should ideally have a fixed wavelength of scattered light with high intensity. From these perspectives, in this study, we developed a method of constructing an optical antenna on the surface of *E. coli* O26 cells using antibody-introduced NSs.

Experimental

Materials and reagents

All chemicals were of reagent grade. Ultrapure water (>18 MΩ cm) sterilized using UV light was used in all experiments. Aniline and glutaraldehyde (GA) were purchased from FUJIFILM Wako Pure Chemical Co. (Japan). Hydrogen tetrachloroaurate(III) tetrahydrate was procured from Tanaka Kikinzoku Kogyo K.K. (Japan). Large AuNPs (Gold nanoparticles, 100 nm in diameter) were purchased from Merck KGaA (Germany). *E. coli* O14:K7 was purchased from American Type Culture Collection (ATCC, Manassas, VA, USA). *Salmonella enterica* was purchased from the National Institute of Technology and Evaluation Biological Resource Center (NBRC, Japan). Genetically modified verotoxin-nonproducing *E. coli* PV01-198 (O26:H11) was provided by Prof. M. Miyake (Department of Veterinary Science, Osaka Prefecture University, Japan) and Dr K. Seto (Osaka Prefectural Institute of Public Health, Japan). The antibodies were obtained from Kirkegaard & Perry Laboratories, Inc.

Bacterial culture and sample preparation

A bacterial strain was cultured in agar growth medium (E-MC35, Eiken Chemical Co., Japan) at 303 K for 48 h. Colonies were suspended in the liquid growth medium (25 mL) and cultured at 303 K for 17 h. After centrifugation at 2,000 ×*g* for 5 min, the supernatant was removed and the precipitate was suspended in ultrapure water by agitating for 1 min. Subsequently, the suspension was centrifuged again using the same conditions mentioned above. These procedures were repeated three times. In the following experiments, the suspension was diluted with ultrapure water to obtain a bacterial concentration of 3.0×10^7 cells mL^{-1}.

Preparation of metal-organic NSs

The metal-organic NSs were prepared in an aqueous solution, as follows: An aqueous aniline solution (0.10 M, 4.0 mL) was added to an aqueous solution of tetrachloroaurate (0.0030wt%, 200 mL), stirred at 353 K for 20 min, and then centrifuged at 8,480 ×*g* and 278 K for 30 min.[22,23] The supernatant was removed, and the precipitate was dispersed in 20 mL of ultrapure water. This procedure was repeated thrice to remove unreacted Au seeds and finally obtain gold-aniline NSs (AuNSs). The final precipitate was dispersed in 20 mL of ultrapure water (0.11 mg mL^{-1}) and stored at room temperature until use.

Aggregation of the AuNSs

An aqueous solution of GA (2.8 M, 2.0 mL) was added to the AuNS suspension (10 mL) and stirred at 298 K.[24] The resultant suspension was subsequently centrifuged at 8,480 ×*g* and 278 K for 30 min. The supernatant was removed, and the precipitate was dispersed in 10 mL of ultrapure water. The procedure was repeated twice to remove unreacted GA. The final precipitate was dispersed in 10 mL of ultrapure water (0.11 mg mL^{-1}). The size distribution of the composite was determined using a zeta potential and particle size analyzer (ELSZ-2Plus, Otsuka Electronics, Japan). Then, 1.0 µL aliquots of the dispersion were pipetted onto ITO glass slides and dried at room temperature for 30 min. The obtained slides were used for microscopic observation using a DFM and FE-SEM.

Immobilization of the antibody on NSs

N-hydroxysuccinimide sodium salt (NHS, 10 mg mL^{-1}) was added to the prepared AuNS suspension (1.0 mL), and the mixture was stirred at 298 K for 30 min. The anti-*E. coli* O26 antibody (1.0 mg mL^{-1}) was added to an aqueous 1-ethyl-3-(3-dimethylaminopropyl) carbodiimide hydrochloride (EDC, 10 mg mL^{-1}) solution and the mixture was stirred for 30 min.[25] The two mixtures obtained above were mixed and stirred for 2 h. The mixture was centrifuged at 6,790 ×*g* and 278 K for 20 min. The supernatant was discarded, and the precipitate was dispersed in 1.0 mL of ultrapure water.

Immobilization of the antibody on the aggregated NSs

The anti-*E. coli* O26 antibody (1.0 mg mL^{-1}, 50 µL) was added to the AuNS aggregate suspension (1.0 mL) and the mixture was stirred at 298 K for 2 h. The resultant mixture was centrifuged at 6,790 ×*g* and 278 K for 20 min. The supernatant was discarded, and the precipitate was dispersed in 1.0 mL of ultrapure water. Then, the supernatant was discarded again, and the precipitate was dispersed in 1.0 mL of ultrapure water.

Microscopic observation

A mixture of the antibody-immobilized AuNS suspension (200 µL) and bacterial suspension (50 µL) was agitated at 298 K for 30 min. Then, 1.0 µL aliquots of the mixture were pipetted onto glass slides and dried at 298 K for 30 min. The obtained slides were used for microscopic observation using a DFM. DFM detected only the light scattered by the sample, while the directly transmitted light was blocked using a dark-field condenser. DFM images were acquired using an optical microscope (Eclipse 80i, Nikon, Japan) with a dark-field condenser, 100 W halogen lamp, and a charge-coupled device camera. The light scattering spectra were recorded using a miniature grating spectrometer (USB4000, Ocean Optics) connected to the DFM using an optical fiber (core diameter, 400 µm).

Results and discussion

Light scattering characteristics of the AuNSs

We constructed a reaction system to automatically control particle formation and formed metal-organic NSs with a uniform size.[22,23] AuNSs showed a raspberry-like structure with a mean diameter of 97±27 nm (Fig. 1A). Each AuNS consisted

ARTICLE

of many AuNPs with an average particle size of 5 nm encapsulated in polyaniline particles. Many non-contacting AuNPs in the polyaniline matrix individually absorb incident light and generate LSPRs.[14,21,24] The LSPR is enhanced owing to the coupling between many adjacent non-contacting AuNPs present within the raspberry structure, resulting in a strong
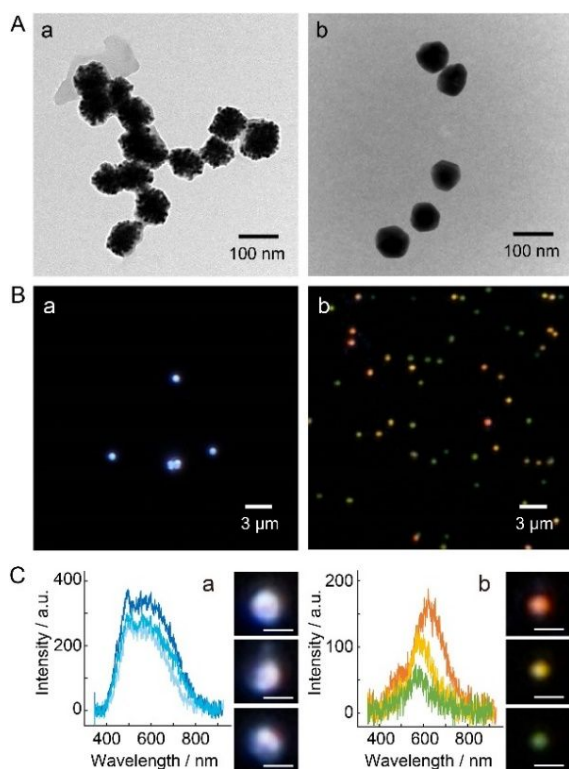

Fig. 1 (A) TEM, (B) DFM images, and (C) light scattering spectra of (a) AuNSs and (b) AuNPs. DFM images were acquired at an exposure time of 100 ms and 100× magnification. Spectral acquisition times were 300 ms. Scale bars in (C) are 1 μm.

whitish scattered light (Fig. 1B). All AuNS particles deposited on the glass slide were observed as whitish light scattering spots in the dark field. In comparison, a single AuNP (commercial sample) with a mean diameter of 100 nm was observed as a greenish, yellowish, or reddish light scattering spot. In general, it is difficult to obtain large and uniform metal particles, and larger NPs have a wider particle size distribution. Therefore, the wavelength of light scattered by these particles differs according to the particle size, and such NPs are not suitable as labels. Using them as labels would require additional size-sieving operations such as centrifugation and filtration. Commercially available AuNPs treated as described above have a uniform particle size (mean diameter: 92±20 nm), but it was observed as various scattered light spots due to their aggregation on the slide (Fig. 1C). Meanwhile, a single AuNS on a glass slide was observed as a whitish light scattering spot under the DFM, regardless of aggregation or dispersion.[21] A comparison of the light scattering spectra of the AuNSs and AuNPs indicated that the light scattering intensity of a single AuNS was 4 times higher than that of an AuNP of the same size. These light scattering particles are useful as labels because the intensity of the scattered light changes according

to the aggregation state of the NS without any color change. Thus, our synthetic method, which uses aniline as the reducing agent, provided AuNSs with a uniform particle size without additional size-sieving, and the light scattering intensity of the AuNS was higher than that of an individual metal nanoparticle of the same size. In our previous study, it was found that the small AuNPs in AuNS fused to form one large AuNP by electrolysis in an alkaline
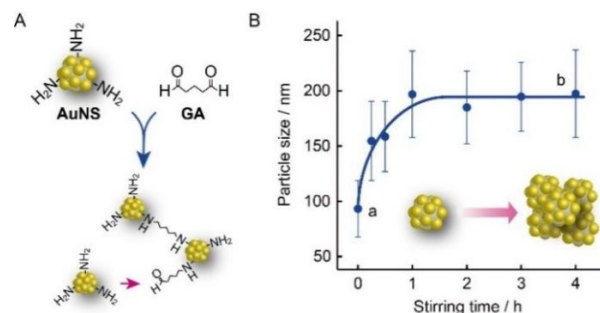

Fig. 2 (A) Illustration of cross-linking between AuNSs using GA. (B) Relationship between the particle size of AuNS aggregates and the reaction time for cross-linking. GA (2.8 M, 2.0 mL) was added to the AuNS suspension (0.11 mg mL^{-1}, 10 mL).

electrolyte. The electrochemical fusion of small AuNPs produced one AuNP with a mean diameter of 73 nm corresponding to the volume of 2.0×10^{-16} cm^3 in a single AuNS.[26] The AuNS was estimated to consist of approximately 3,000 small AuNPs with a mean diameter of 5 nm corresponding to the volume of 6.5×10^{-20} cm^3.[22] Further, a comparison of the light scattering properties of the AuNS and AuNP of the same size suggested that the scattered light intensity was enhanced by the coupling of the LSPRs of adjacent AuNPs in the AuNS consisting of small NPs.[14,21,24] These effects demonstrate the potential of the AuNS as an optical label that can provide high scattering intensity despite the use of a small amount of the noble metal, Au. Therefore, in the detection of bacteria using the AuNSs as labels, a more sensitive detection could be achieved.

We investigated the possibility of increasing the sensitivity of the as-prepared AuNS further as a label. To obtain a more effective label, we attempted to control the aggregation of the AuNSs using GA as a cross-linking agent, which helped to form uniform aggregated structures of large sizes (Fig. 2A).[25] GA, which has two aldehyde groups, reacts with an amino group to crosslink AuNS. When GA was mixed with the AuNS suspension, NS aggregated as the cross-linking reaction progressed. The aggregate size increased with an increase in the stirring time and eventually reached a constant value after 1 h of stirring (Fig.
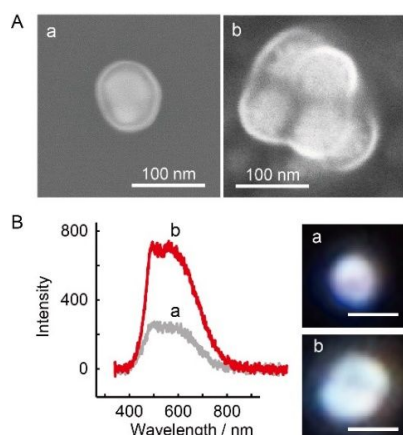
Fig. 3 (A) FE-SEM, (B) DFM images and light scattering spectra of AuNSs (a) before and (b) after their reaction with GA for 4 h. DFM images and light scattering spectra of AuNSs were obtained on glass slides. DFM images were acquired at an exposure time of 1 s and 100× magnification. Spectral acquisition times were 300 ms. Scale bars in (B) are 1 μm.

2B). The size of the aggregates was measured to be 197±40 nm using a particle size analyzer after a cross-linking reaction time of 4 h. The light scattering intensity of the aggregate was observed with a variation of ± 20% depending on the size distribution.

SEM observations revealed that most of the aggregates consisted of four to five AuNS particles (Fig. 3A&Fig. S1). The light scattering intensity of the aggregates was approximately three times higher than that of a single AuNS (Fig. 3B). Every aggregate generated a strong whitish scattered light spot without any color change. This result implies that the enhancement of light scattering due to LSPR coupling observed in a single AuNS was maintained even when the AuNSs were aggregated. Furthermore, the aggregation of the AuNSs could be controlled by optimizing the stirring time at a given GA:AuNS ratio. The aggregation of the AuNSs is expected to contribute to an increase in the sensitivity of bacterial detection. However, the steric hindrance of bulky aggregates (average diameter, 200 nm) bound to bacterial cells might inhibit the binding of other new aggregates to the antigens.

The specific binding property of the AuNSs

We attempted to label specific bacterial cells with AuNSs to exploit the scattering properties of AuNSs in targeted bacterial detection. The amount of GA affected the rate of the aggregation reaction and did not affect the final size of the aggregate (Fig. S2). In other words, it was speculated that the unreacted aldehyde groups retained on the surface of the aggregates when an excess amount of GA was added. As GA was present on the surface of AuNSs to adjust the particle size through aggregation, the introduction of antibodies was easily realized through simple mixing of the aggregated NSs with the antibody. Other aldehyde groups of GA on the surface of AuNS bound to amino groups of the antibody. In contrast, the introduction of antibodies into unaggregated single NSs required the use of the NHS and EDC system.[21] Subsequently, each of the labels (individual and aggregated AuNSs attached with antibodies) was mixed with *E. coli* O26 as an antigen and

then observed under a DFM. The labeled *E. coli* O26 cells were observed as strong light scattering spots, whereas the unlabeled cells appeared as weak light spots (Fig. 4). Comparison of the light scattering intensities indicated that the cells labeled with small AuNSs (Fig. 4a) yielded approximately 2.5 times stronger light intensity than the unlabeled ones (Fig. 4d). As the size of the label increased, the scattered light from the labeled *E. coli* O26 cell became more intense, and the scattered light intensity of a single cell labeled with aggregated NSs at 600 nm was enhanced by up to 5.2 folds compared to that of an unlabeled cell. On the other hand, the antibody-immobilized AuNPs having a mean diameter of 11 ± 2.1 nm increased the light scattering intensity of cells by only approximately 1.5 times that of unlabeled ones. Similarly, fluorescent labels using dye-binding antibodies can specifically detect the target cells, but require at least 1 s of exposure time to obtain sufficient fluorescence intensity to clearly observe the cells. However, we were able to obtain sufficient light scattering intensity to clearly identify the
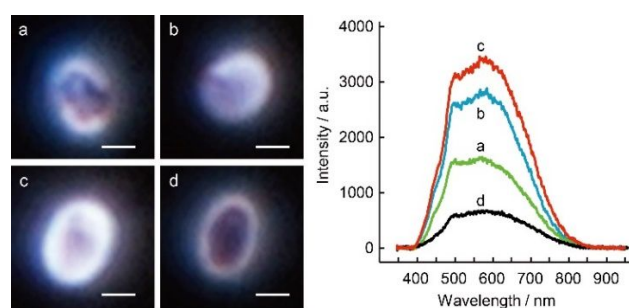

Fig. 4 DFM images and light scattering spectra of *E. coli* O26 (a–c) with and (d) without antibody-immobilized NS labeling on glass slides. Mean diameters were 107 nm (a), 208 nm (b) and 242 nm (c), respectively. Image acquisition times in dark-field observations were 100 ms and spectrum acquisition times were 300 ms. Scale bars are 1 μm.

target cells with an exposure time of 100 ms in dark-field observation. Therefore, the use of large particles as labels is expected to increase the visibility in the observation of bacterial cells. Although the scattering strength of the AuNS label increased by three folds after its aggregation, the light scattering intensity in bacterial detection was enhanced only by approximately 2.1 folds. This fact indicates that the bulky aggregates bound to bacterial cells caused steric hindrance and suppressed the binding of other new aggregates to the antigens. On the other hand, as the particle size of the aggregates increases, the number of AuNS bound to the bacterial cell increased and the light scattering intensity of the labeled cell increased. The variation of ± 20% observed in the light scattering intensity of the aggregate was reflected to those of the labeled cells. This indicates that the aggregate containing this variation acts as a highly reproducible label. There was no change in the color of the scattered light spot before and after labeling. This implies that the spectrum of the labeled cell could be considered as the sum of the spectra of the cells and labels.
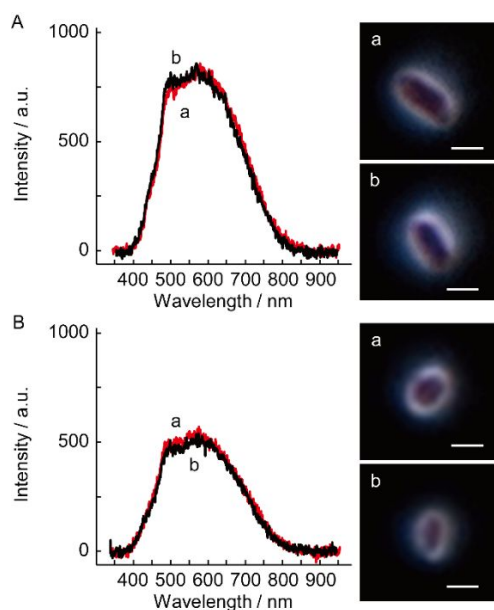
ARTICLE

Fig. 5 DFM images and light scattering spectra of (A) *E. coli* O14 and (B) *S. enterica* (a) with and (b) without anti-O26 antibody-immobilized AuNSs on glass slides. Image acquisition times in dark-field observations were 100 ms and spectral acquisition times were 300 ms. Scale bars are 1 µm.

That is, both unlabeled and labeled cells were observed as white light spots, but the labeled cells were observed as stronger white light spots. Thus, the image observed in the dark field was consistent with the qualitative and quantitative information of the intensity and wavelength obtained from the light scattering spectra.

Selective binding is as important as sensitivity in the detection of a single bacterium. Specific labeling can be realized by introducing an antibody into the AuNS to enable the binding of the antibody-introduced AuNS to an antigen on the surface of the targeted bacterium. The performance of antibodies and non-specific adsorption are key factors that cause false negatives and false positives. Therefore, we evaluated the binding properties of the antibody-introduced AuNSs. The labeled cells could be observed as light spots based on the characteristic light scattering of AuNSs under a DFM, because the antibodies bound to specific antigens on the cell surface (see Fig. 4). Moreover, it was confirmed that the AuNS labels did not bind to the mismatching bacterial cells that had different antigens on their surfaces (Fig. 5).

Many unbound AuNSs were observed on the glass slide when other strains of bacteria were mixed with the AuNS label containing a specific antibody. Thus, we confirmed the specific binding properties of the antibody-introduced AuNS. The binding properties of the antibody immobilized on the AuNS made it possible to label the corresponding bacterial cells, enabling specific detection based on light scattering.

Validation using a real sample

Given the success of our initial tests, we further evaluated the ability of our AuNSs to detect *E. coli* O26 cells in real sample suspensions extracted from a rotten chicken. The real sample suspensions obtained from the rotten chicken contained various viable bacteria (total cell count, 6.5×10^4 cells mL^{-1})

such as lactic acid bacteria (1.0×10^4 cells mL^{-1}), *E. coli* (< 10 cells mL^{-1}) and others, but not enterohemorrhagic *E. coli* as analyzed by Falco Biosystems Co., Ltd. (Kyoto, Japan). The target *E. coli* O26 cells were added to the real sample suspension to a concentration of 13% of the total cell count. After the addition of the anti-*E. coli* O26 antibody-immobilized AuNSs to the suspension, 1.0 µL of the mixture was dropped onto a glass slide and observed in dark field. In the sample with added *E. coli* O26, we observed some strong oval light scattering spots that
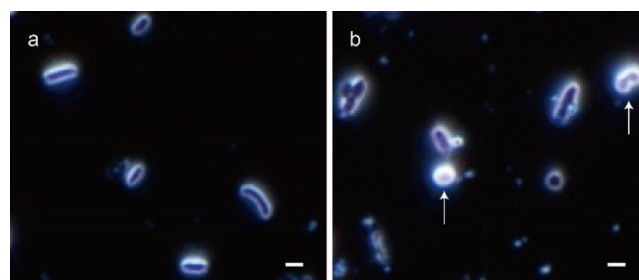

Fig. 6 DFM image and light scattering spectra of bacterial cells labeled (a) with and (b) without anti-E. coli O26 antibody-immobilized AuNS and other unlabeled bacterial cells in a real rotten minced chicken sample. The positions of labeled cells are indicated by arrows. Image acquisition times in dark-field observations were 100 ms. Scale bars are 1 µm.

coincided with the AuNS-labeled *E. coli* O26 cells (Fig. 6).[27] The strong light scattering spots constituted 11.4±1.6% of the total scattering spots, in good agreement with the occupancy rate of the loaded *E. coli* O26 cells (13%) in the real sample suspension.

Conclusions

An AuNS provides stronger scattered light intensity than an AuNP of the same particle size and is useful as a label because the scattered light has a stable white color, regardless of its aggregation state. As the size of the AuNS aggregated using GA increases, the scattered light intensity increases without a change in the wavelength of the scattered light. This is useful for achieving high sensitivity and excellent visibility with its use as a label. The antibody-immobilized AuNS label does not bind to mismatched bacteria owing to the specific binding properties of the antibody, and can specifically detect the target bacterium. In addition, we were able to label the target cells in a real sample. Similarly, fluorescent labels using dye-binding antibodies can specifically detect target bacteria, but their short fluorescence lifetime raises concerns about intensity reproducibility. However, it can be expected that the detection based on the light scattering characteristics will be highly reproducible since the NSs are chemically stable. Thus, we demonstrated that AuNSs can act as sensitive optical nanoantenna that are suitable for rapid cell detection.

Author contributions

S.I. and S.T. conducted the experiments, analyzed the data, and wrote the manuscript. H.I., M.Y., Y.T., K.Y., X.S., S.N. and

Y.Y. conducted the experiments and analyzed the data. Y.S., Z.C. and H.S. designed and supervised the experiments, analyzed the data, and wrote the manuscript.

Conflicts of interest

There are no conflicts to declare.

Acknowledgments

References

1   A. G. Atanasov, S. B. Zotchev and V. M. Dirsch, *Nat. Rev. Drug Discov*., 2021, **20**, 200.

2   M. Saarela, G. Mogensen, R. Fondén, J. Mättö and T. M. Sandholm, *J. Biotech*., 2000, **84**, 197.

3   J. B. Kaper, J. P. Nataro and H. L. Mobley, *Nat. Rev. Microbiol*., 2004, **2**, 123.

4   F. R. Blattner, G. Plunkett III, C. A. Bloch, N. T. Perna, V. Burland, M. Riley, J. Collado-Vides, J. D. Glasner, C. K. Rode, G. F. Mayhew, J. Gregor, N. W. Davis, H. A. Kirkpatrick, M. A. Goeden, D. J. Rose, B. Mau, Y. Shao, *Science*, 1997, **277**, 1453.

5   J. P. Nataro and J. B. Kaper, *Clin. Microbiol. Rev.*, 1998, **11**, 142.

6   T. Hayashi, K. Makino, M. Ohnishi, K. Kurokawa, K. Ishii, K. Yokoyama, C. G. Han, E. Ohtsubo, K. Nakayama, T. Murata, M. Tanaka, T. Tobe, T. Iida, H. Takami, T. Honda, C. Sasakawa, N. Ogasawara, T. Yasunaga, S. Kuhara, T. Shiba, M. Hattori, H. Shinagawa, *DNA Res.*, 2001, **8**, 11.

7   R. A. Welch, V. Burland, G. Plunkett III, P. Redford, P. Roesch, D. Rasko, E. L. Buckles, S.-R. Liou, A. Boutin, J. Hackett, D. Stroud, G. F. Mayhew, D. J. Rose, S. Zhou, D. C. Schwartz, N. T. Perna, H. L. T. Mobley, M. S. Donnenberg, and F. R. Blattner, *Proc. Natl. Acad. Sci. USA*, 2002, **99**, 17020.

8   H. Shiigi, *Anal. Sci.*, 2019, **35**, 235.

9   J. H. Warcup, *Trans. Brit. Mycol. Soc.*, 1955, **38**, 298.

10 S. Hameed, L. Xie, Y. Ying, *Trends Food Sci. Technol.,* 2018, **81**, 61.

11 H. C. Gram, *Fortschr. Med.*, 1884, **2**, 185.

12 M. J. Wilhelm, J. B. Sheffield, M. Sharifian Gh., Y. Wu, C. Spahr, G. Gonella, B. Xu, and H.-L. Dai, *ACS Chem. Biol.*, 2015, **10**, 1711.

13 M. Berney, F. Hammes, F. Bosshard, H. U. Weilenmann, T. Egli, *Appl. Environ. Microbiol.*, 2007, **73**, 3283.

14 H. Shiigi, M. Fukuda, T. Tono, K. Takada, T. Okada, L. Dung, Y. Hatsuoka, T. Kinoshita, M. Takai, S. Tokonami, H. Nakao,

T. Nishino, Y. Yamamoto and T. Nagaoka, *Chem. Commun.,* 2014, **50**, 6252.

15 T. Kinoshita, K. Kiso, D. Q. Le, H. Shiigi, T. Nagaoka, *Anal. Sci.*, 2016, **32**, 301.

16 G. P. Acuna, F. M. Möller, P. Holzmeister, S. Beater, B. Lalkens, P. Tinnefeld, *Science*, 2012, **338**, 506.

17 A. Moreau, C. Ciracì, J. J. Mock, R. T. Hill, Q. Wang, B. J. Wiley, A. Chilkoti, D. R. Smith, *Nature*, 2012, **492**, 86.

18 K. Ishiki, K. Okada, D. Q. Le, H. Shiigi, T. Nagaoka, *Anal. Sci.*, 2017, **33**, 129.

19 K. Ishiki, H. Shiigi, T. Nagaoka, *Anal. Sci.*, 2017, **33**, 551.

20 W. P. Faulk and G. M. Taylor, *Immunochemistry*, 1971, **8**, 1081.

21 H. Shiigi, T. Kinoshita, M. Fukuda, D. Q. Le, T. Nishino and T. Nagaoka, *Anal. Chem.*, 2015, **87**, 4042.

22 H. Shiigi, Y. Yamamoto, N. Yoshi, H. Nakao and T. Nagaoka*, Chem. Commun*., 2006, 4288.

23 H. Shiigi, R. Morita, Y. Yamamoto, S. Tokonami, H. Nakao, T. Nagaoka, *Chem. Commun.*, 2009, 3615.

24 T. Kinoshita, D. Q. Nguyen, T. Nishino, H. Nakao, H. Shiigi, T. Nagaoka, *Anal. Sci.*, 2015, **31**, 487.

25 D. Q. Nguyen, K. Ishiki, H. Shiigi, *Microchimica Acta*, 2018, **185**, 465.

26 H. Shiigi, Y. Muranaka, Y. Hatsuoka, Y. Yamamoto and T. Nagaoka, *J. Electrochem. Soc.,* 2013, **160**, H813.

27 S. Tanabe, S. Itagaki, S. Sun, K. Matsui, T. Kinoshita, S. Nishii, Y. Yamamoto, Y. Sadanaga, H. Shiigi, *Anal. Sci.*, 2021, **37**, 1597.